

A Highly Sensitive and Fast-Responding SnO₂ Sensor Fabricated by Combustion Chemical Vapor Deposition

Ying Liu, Erik Koep, and Meilin Liu*

Center for Innovative Fuel Cell and Battery Technologies, School of Materials Science and Engineering,
Georgia Institute of Technology, Atlanta, Georgia 30332-0245

Received February 27, 2005. Revised Manuscript Received May 20, 2005

Highly porous and nanostructured SnO₂ thin-film gas sensors with Pt interdigitated electrodes have been fabricated via a combustion chemical vapor deposition process. The SnO₂ films were less than 1 μm thick and consisted of nanocrystallites smaller than 30 nm. At 300 °C, the as-prepared SnO₂ gas sensor showed a sensitivity of 1075 to 500 ppm ethanol vapor, and the corresponding response time and recovery time were 31 and 8 s, respectively. The extrapolated low detection limit appears to be below 1 ppm. Consequently, the as-fabricated sensor demonstrated significant improvements over those reported in the literature. These highly sensitive, fast-responding, and low-cost SnO₂ sensors could have many practical applications.

Introduction

Highly sensitive and reliable gas sensors are vital to many applications such as monitoring and control of air quality, detection of flammable or toxic gases, electronic noses, medical diagnosis, and optimization of combustion efficiency. Tin dioxide is an n-type semiconductor widely used for gas sensors. The gas detection mechanism is based on the reversible change in conductivity of the surface of SnO₂ particles/grains induced by gas–solid interaction.¹ Several strategies have been adopted to enhance the performance of SnO₂ gas sensors, including doping with aliovalent ions (e.g., Cu, Zn,² In³), catalytically active additives (e.g., Pt and Pd),^{4,5} and addition of carbon nanotubes.⁶

Further, it is well known that gas-sensing characteristics of SnO₂ can be dramatically altered by morphological and microstructural features of the sensing elements such as particle size, shape, surface/volume ratio, and porosity. Ultrathin films, porous films, and more recently, nanocrystalline films of SnO₂ have been fabricated by a variety of approaches, such as evaporative methods,^{7,8} sputtering,^{9,10} chemical vapor processes,¹¹ and chemical solution tech-

niques.^{12,13} Many of these techniques suffer from one or more drawbacks such as low deposition rate, prolonged postprocess (e.g., annealing) time, and expensive target/precursor and apparatus. Combustion chemical vapor deposition (CVD) is a cost-effective and versatile process capable of producing films with a wide variety of morphologies. Highly porous and nanostructured films have been synthesized for energy storage and conversion applications such as solid oxide fuel cells and batteries.^{14,15} In this article, we report a nanostructured, thin-film SnO₂ gas sensor with interdigitated Pt electrodes fabricated using a cost-effective combustion CVD process. The extremely porous SnO₂ thin film demonstrated exceptionally high sensitivity and fast speed of response and recovery upon exposure to ethanol vapor.

Experimental Section

Platinum interdigitated electrodes were fabricated on 25.4 mm \times 76.2 mm quartz slides. Titanium (20 nm in thickness) was deposited on quartz slides to improve the adhesion of metals on the substrates. The platinum was then deposited by direct current (DC) sputtering over the thin titanium layer. The patterned platinum electrode stripes are 10 μm wide, and the spacing between two adjacent electrode stripes is 10 μm . There were in total 40 stripes on each pattern. Approximately 20 patterned electrodes were fabricated on each quartz slide and were cut into individual pieces (4 mm \times 10 mm) after fabrication.

SnO₂ thin-film gas sensors were deposited on patterned platinum electrodes using a combustion CVD process, which has been employed to fabricate many novel nanostructures and devices recently.^{14,15} Precursor solution was prepared by dissolving tin(II) 2-ethylhexanoate (Aldrich) in absolute ethanol. Deposition was carried out at 850 °C for 20 min. For structural analysis, an X-ray

* To whom correspondence should be addressed. Phone: 404-894-6114. Fax: (+1) 404-894-9140. E-mail: meilin.liu@mse.gatech.edu.

- (1) Tiburcio-Silver, A.; Sánchez-Juárez, A. *Mater. Sci. Eng. B* **2004**, *110*, 268.
- (2) Yu, J. H.; Choi, G. M. *Sens. Actuators, B* **2001**, *75*, 56.
- (3) Salehi, A. *Thin Solid Films* **2002**, *416*, 260.
- (4) Schweizer-Berberich, M.; Zheng, J. G.; Weimar, U.; Göpel, W.; Bárán, N.; Pentia, E.; Tomescu, A. *Sens. Actuators, B* **1996**, *31*, 71.
- (5) Bittencourt, C.; Llobet, E.; Ivanov, P.; Correig, X.; Vilanova, X.; Brezmes, J.; Hubalek, J.; Malysz, K.; Pireaux, J. J.; Calderer, J. *Sens. Actuators, B* **2004**, *97*, 67.
- (6) Wei, B. Y.; Hsu, M. C.; Su, P. G.; Lin, H. M.; Wu, R. J.; Lai, H. J. *Sens. Actuators, B* **2004**, *101*, 81.
- (7) Madhusudhana Reddy, M. H.; Chandorkar, A. N. *Sens. Actuators, B* **1992**, *9*, 1.
- (8) Banerjee, R.; Das, D. *Thin Solid Films* **1987**, *149*, 291.
- (9) Choe, Y. S. *Sens. Actuators, B* **2001**, *77*, 200.
- (10) Min, B. K.; Choi, S. D. *Sens. Actuators, B* **2004**, *98*, 239.
- (11) Murty, N. S.; Jawalekar, S. R. *Thin Solid Films* **1983**, *102*, 283.

- (12) Rosental, A.; Tarre, A.; Gerst, A.; Uustare, T.; Sammelselg, V. *Sens. Actuators, B* **2001**, *77*, 297.
- (13) Nayral, C.; Ould-Ely, T.; Maisonnat, A.; Chaudret, B.; Fau, P.; Lescouzères, L.; Peyre-Lavigne, A. *Adv. Mater.* **1999**, *11*, 61.
- (14) Liu, Y.; Zha, S.; Liu, M. *Adv. Mater.* **2004**, *16*, 256.
- (15) Liu, Y.; Zha, S.; Liu, M. *Chem. Mater.* **2004**, *16*, 3502.

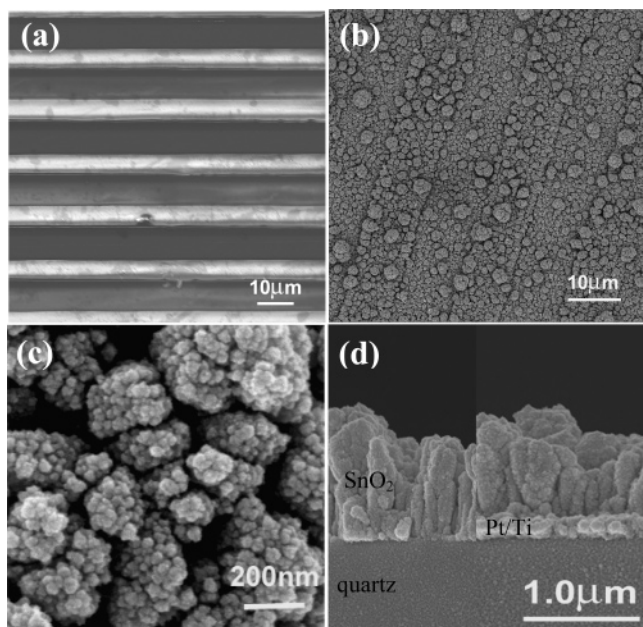


Figure 1. (a) SEM image of platinum interdigitated electrodes with a strip width of 10 μm and line space of 10 μm . (b) Top view of nanostructured SnO_2 gas sensor fabricated at 850 $^\circ\text{C}$ by a combustion CVD process. (c) Higher magnification SEM micrograph of SnO_2 thin film, showing each individual particle is less than 30 nm. (d) Cross-sectional view of SnO_2 sensor. The left portion shows SnO_2 thin film directly deposited on quartz substrate, while the right part shows SnO_2 film grown on Pt electrode.

diffraction (XRD) sample was prepared on a clear quartz slide without Pt electrodes under identical conditions.

The structure and morphology of the as-prepared samples were characterized using an X-ray diffractometer (XRD, Phillips PW 1800) and scanning electron microscope (SEM, LEO 1530 thermally assisted FEG).

Ethanol-sensing tests were conducted in a tube furnace from 200 to 500 $^\circ\text{C}$ at a 50 $^\circ\text{C}$ interval. Dry air and air–ethanol vapor mixture were delivered to the furnace via a three-way valve at a constant rate of 100 sccm. The current flowing through the SnO_2 sensor was registered using a Solartron 1285 potentiostat interfaced with a PC at an applied constant voltage of 100 mV. Initially, tests were conducted from 200 to 500 $^\circ\text{C}$ using a constant ethanol vapor concentration of 500 ppm. Once the temperature of highest sensitivity was identified, experiments were carried out at that temperature using ethanol vapor from 50 to 500 ppm.

Results and Discussion

Shown in Figure 1a is an SEM image of Pt interdigitated electrodes with a line width of 10 μm and line space of 10 μm . Pt strips are straight and well defined. Figure 1b is a top view of the SnO_2 gas sensor film deposited at 850 $^\circ\text{C}$. The film consists of small particles, most of which are smaller than 1 μm with the exception of some particles as large as 3 μm in diameter. The top-view SEM micrograph also reveals the outline of the Pt interdigitated electrodes, indicating the deposited SnO_2 film is thin and semitransparent. As seen from a higher magnification micrograph of the SnO_2 film, Figure 1c, each individual agglomerate that appears in Figure 1b actually consists of much finer crystals less than 30 nm in diameter. Figure 1d shows a cross-sectional SEM micrograph of the sample. The left portion shows SnO_2 thin films directly deposited on quartz substrate, while the right part shows SnO_2 films grown on a Pt

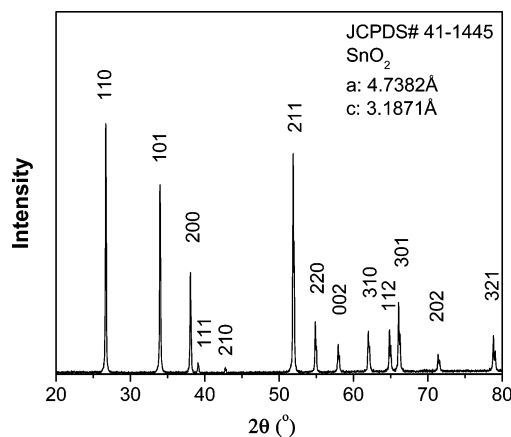


Figure 2. XRD pattern of SnO_2 film fabricated at 850 $^\circ\text{C}$ for 20 min. The SnO_2 thin film is determined to have a tetragonal structure.

electrode. The SnO_2 film is about 1 μm thick, and each grain has a columnar orientation.

Shown in Figure 2 is an XRD pattern for a SnO_2 film sample prepared on a quartz slide under the same deposition condition as for the SnO_2 sensor shown in Figure 1. The intensities and locations of all the peaks match those on JCPDS# 41-1445, confirming the as-deposited SnO_2 film has a tetragonal structure with $a = 4.7382 \text{ \AA}$ and $c = 3.1871 \text{ \AA}$.

The as-prepared SnO_2 films were tested for ethanol sensing behavior from 200 to 500 $^\circ\text{C}$ at 50 $^\circ\text{C}$ intervals. A typical electrical response of the SnO_2 thin film sensor to 500 ppm ethanol vapor at 450 $^\circ\text{C}$ is shown in Figure 3a. Initially, the current flowing through the sample under a constant DC voltage of 100 mV was trivial (about $2.2 \times 10^{-6} \text{ A}$). Upon exposure to ethanol vapor, however, the current passing through the film jumped abruptly and reached a steady plateau in a relatively short period of time. The response behavior followed an exponential correlation. The recovery process mirrored the initial process with similar characteristics, albeit at much higher speed.

Shown in Figure 3b are the Arrhenius plots for the response and recovery time, which is defined as the time needed to reach 90% of total signal change. It took 95 s for the SnO_2 sensor to respond and 26 s to recover at 250 $^\circ\text{C}$. However, the response and recovery time were reduced to 39 and 11 s, respectively, as the operating temperature was raised to 450 $^\circ\text{C}$. Generally, gas sensors made from thin films take less time to reach a saturation plateau than to fully recover. However, for SnO_2 sensors fabricated by combustion CVD, the speed of recovery is actually faster than that of response. Since the sensing material and testing parameters were comparable to those reported in the literature, the fast speed of response/recovery should be attributed to the highly porous and nanostructured morphology of the sensor film.

As shown in Table 1, the response and recovery time are compared with those of SnO_2 sensors fabricated by other approaches. For instance, it took 36–45 s to respond and 300–420 s to recover for a SnO_2 film sensor tested at 275 $^\circ\text{C}$ and 1000 ppm ethanol, while the corresponding characteristic constants for a sensor fabricated by combustion CVD and tested at 300 $^\circ\text{C}$ and 500 ppm were 31 and 8 s, respectively.

Usually, gas sensitivity (S) is expressed as the ratio of electrical resistance in air (R_a) to that in the testing gas (R_g):

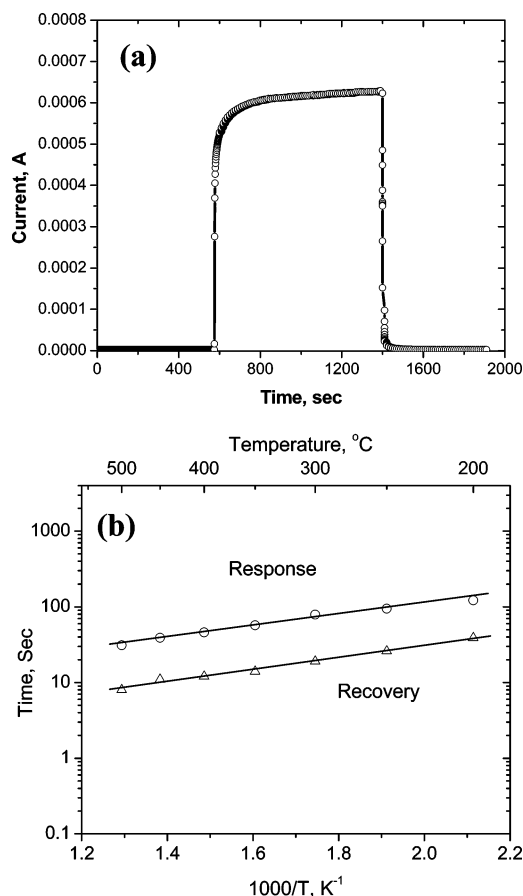


Figure 3. (a) Typical electrical response of a SnO₂ gas sensor to 500 ppm ethanol vapor measured at 450 °C. Open circles on the curve represent the current values acquired at every second. (b) Response and recovery time of the sensor to 500 ppm ethanol vapor as a function of testing temperature from 200 to 500 °C.

Table 1. Comparison of Sensing Characteristics of Pure SnO₂ Gas Sensors Fabricated by Different Approaches

fabrication approach	ethanol concentrated (ppm)	temperature (°C)	sensitivity $S = R_{\text{air}}/R_{\text{gas}}$	response time (s)	recovery time (s)
sol-gel ²³	150	250	3.2		
spin coating ²⁴	400	200	6.2	170	
RT CVD ¹⁸	1000	300	100		
EB evaporation ²⁵	300	300	160		
not specified ²⁶	1000	275	280	36–45	300–420
combustion CVD (this work)	500	200	50.5	122	39
	100	300	280	55	17
	300	300	696	42	12
	500	300	1075	31	8

$S = R_{\text{a}}/R_{\text{g}}$. Sensitivities at different testing temperatures for SnO₂ sensor fabricated using combustion CVD are shown in Figure 4a. At low temperatures, the sensitivity is relatively low (e.g., 50.5 at 200 °C), but it increases very rapidly with temperature. At 300 °C, the sensitivity peaked to its maximum value of 1070. Above 300 °C, sensitivity gradually decreased as the testing temperature increased further. The trend and the most sensitive temperature are in good agreement with data reported in the literature.¹⁶ However, as shown in Table 1, sensitivities at the corresponding individual testing temperatures are dramatically higher than those reported in the literature.

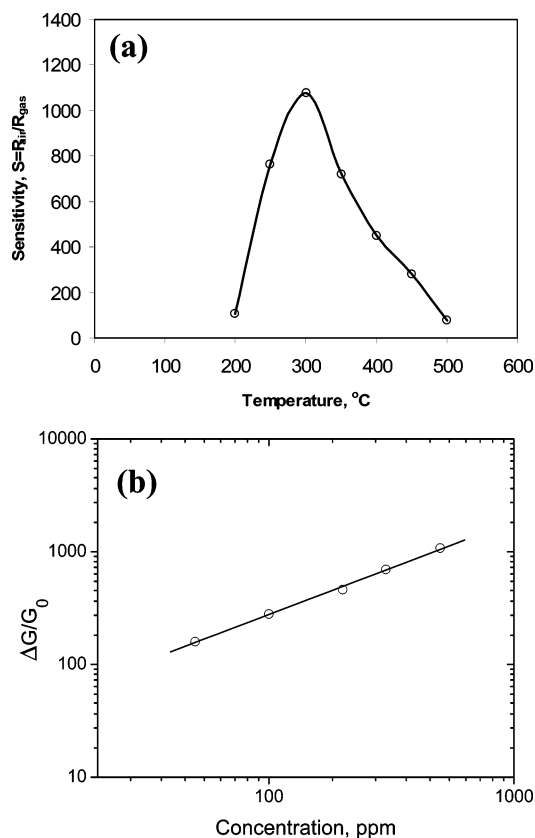


Figure 4. (a) Sensitivity of a SnO₂ sensor fabricated at 850 °C and tested for 500 ppm ethanol at different temperatures. (b) Relative conductance change with ethanol vapor concentrations for a SnO₂ sensor tested at 300 °C.

It is well recognized that the sensing behavior of a thin-film gas sensor is extremely sensitive to grain size and surface conditions. The gas-detecting mechanism of SnO₂ is relevant to the electron-depletion region on the surface of SnO₂ particles/grains created by the preadsorbed surface oxygen. The resulting nonstoichiometry in surface layers leads to a higher energy barrier to electron transport through these regions. The energy barrier can be lowered when the reducing gas species in the surrounding environment interact with the preadsorbed surface oxygen.¹ The smaller the grain size, the higher the surface area and the larger the change in electrical conductivity upon exposure to reducing gas species. For comparison, a porous film gas sensor consisting of large SnO₂ particles showed a sensitivity of 15 when exposed to 100 ppm ethanol at 300 °C,¹⁷ while our sensor with nanosize grains displayed a sensitivity of 280 under the same conditions. The relative conductance changes are also plotted on a logarithmic scale in Figure 4b as a function of ethanol concentration. The ethanol concentration dependence follows the well-known power behavior, $\Delta G/G_0 = A[C_{\text{gas}}]^B$, where C_{gas} is the concentration of the testing gas. If we assume a relative variation in conductance of 40%, the detection limit at 300 °C is 0.05 ppm, a great improvement over current sensing devices. Since an effective breath analyzer must detect at least 200 ppm ethanol corresponding approximately to 0.5 g alcohol/L in the blood,¹⁸ the low detection limit of our sensor improves sensitivity by several orders of mag-

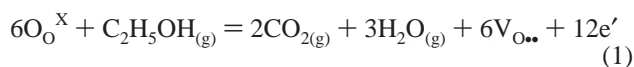
(16) Ihokura, K.; Watson, J. *The Stannic Oxide Gas Sensor: Principles and Applications*; CRC Press: Boca Raton, Florida, 1994.

(17) Ivanov, P.; Llobet, E.; Vilanova, X.; Brezmes, J.; Hubalek, J.; Correig, X. *Sens. Actuators, B* **2004**, 99, 201.

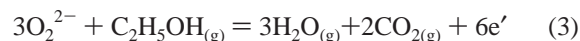
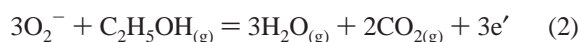
nitude. For 200 ppm ethanol, the relative conductance change at 300 °C is 46000%.

The gas-sensing behavior of a semiconducting oxide can be attributed to both surface and bulk interactions, depending on grain size or film thickness. If the grain size or film thickness is much larger than the Debye length λ_D of the material, the bulk interactions will dominate the sensor response. On the other hand, if the grain size or film thickness is smaller than or in the same order of magnitude as λ_D , surface interactions will dominate the sensor behavior.^{19,20} The large surface-to-volume ratio of the nanostructured SnO₂ thin film suggests that ethanol–SnO₂ interactions on the surface may play an important role.

The interactions between ethanol and lattice oxygen O_O^x in a metal oxide such as SnO₂ can be described in general by the following defect reaction (in Kröger–Vink notation)



Similarly, the interactions between ethanol and the surface-adsorbed oxygen species²¹ such as superoxide ion O₂[−] and peroxide ion O₂^{2−} can be described as



These reactions produce more electrons and thus increase the conductivity of SnO₂ (n-type) upon exposure to ethanol. The dependence of conductivity on partial pressure of ethanol can be derived from these reactions using mass-action law and charge neutrality relations. This will be further investigated in subsequent studies.

The retarded recovery speed for most existing gas sensors makes them inconvenient for practical use, since either much longer waiting time or higher temperature is required for full recovery. The SnO₂ thin layers deposited via combustion CVD show dramatically improved surface interaction with gas molecules as indicated by the short response time and, more particularly, the super-fast recovery speed for ethanol vapor. This behavior can be tentatively justified by assuming that nanosized particles imply much higher surface areas,

porosity, and stronger bonding between particles as well. While the detailed mechanism for the superior ethanol-sensing performance of the thin film SnO₂ sensor is yet to be confirmed, the interdigitated nanoporous sensor may have significant scientific and technological implications: This makes combustion vapor phase deposited sensors quite interesting for many potential applications such as food quality control,²² alcohol identification, electronic noses, and medical diagnosis. The ultralow detection limit (<1 ppm) and high sensitivity offer unique options for cost-effective sensors with a greatly improved level of reliability. Combustion CVD presents a cost-effective technique easily scaled up for quick manufacturing of fast acting, highly sensitive, and reliable gas sensors. Further, the sensor can be miniaturized, which is essential to the development of integrated and smart systems with compact volume and less power consumption. The sensor can also be fabricated in arrays and integrated with a signal-processing unit to further enhance the sensitivity and selectivity.

Conclusions

In summary, highly porous and nanostructured SnO₂ thin film gas sensors with Pt interdigitated electrodes have been fabricated via a combustion CVD process. The SnO₂ films were less than 1 μm thick and consisted of nanocrystallines smaller than 30 nm. The as-prepared SnO₂ gas sensors have been tested for ethanol vapor sensing behavior in the temperature range of 200–500 °C. At 300 °C, the sensitivity to 500 ppm ethanol vapor was 1075 while the corresponding response time and recovery time were 31 and 8 s, respectively. The extrapolated low detection limit seems to be below 1 ppm. Consequently, the as-fabricated sensor demonstrated significant improvements over those reported in the literature. These highly sensitive, fast-responding, and low-cost SnO₂ sensors could have many practical applications.

Acknowledgment. This work was supported by the Center for Innovative Fuel Cell and Battery Technologies, Georgia Institute of Technology.

CM050451O

- (18) Ho, J. J.; Fang, Y. K.; Wu, K. H.; Hsieh, W. T.; Chen, C. H.; Chen, G. S.; Ju, M. S.; Lin, J. J.; Hwang, S. B. *Sens. Actuators, B* **1998**, *50*, 227.
 (19) Radecka, M.; Zakrzewska, K.; Rekas, M. *Sens. Actuators, B* **1998**, *47*, 194.
 (20) Barsan, N.; Weimar, U. *J. Electroceram.* **2001**, *7*, 143.
 (21) Schierbaum, K. D. *Sens. Actuators, B* **1989**, *18*, 71.

- (22) Huang, X.; Liu, J.; Shao, D.; Pi, Z.; Yu, Z. *Sens. Actuators, B* **2003**, *96*, 630.
 (23) Rella, R.; Serra, A.; Siciliano, P.; Vasanelli, L.; De, G.; Licciulli, A.; Quirini, A. *Sens. Actuators, B* **1997**, *44*, 462.
 (24) Weber, I. T.; Andrade, R.; Leite, E. R.; Longo, E. *Sens. Actuators, B* **2001**, *72*, 180.
 (25) Mo, Y.; Okawa, Y.; Nakai, T.; Tajima, M.; Natukawa, K. *Thin Solid Films* **2002**, *416*, 248.
 (26) Wang, Y.; Wu, X.; Li, Y.; Zhou, Z. *Solid-State Electron.* **2004**, *48*, 627.